Intense-field zero-width resonances and control of molecular photodissociation

O. Atabek* and R. Lefebvre†
Laboratoire de Photophysique Moléculaire du CNRS, Université Paris-Sud, Bâtiment 210, Campus d'Orsay 91405, Orsay, France

C. Lefebvre‡ and T. T. Nguyen-Dang§
Département de Chimie, Université Laval, Québec, Québec, Canada G1K 7P4
(Received 21 February 2008; published 22 April 2008)

An efficient and selective laser-induced molecular stabilization with respect to dissociation is obtained by an appropriate shaping of an intense ultraviolet-visible laser pulse which ensures the adiabatic transport of the system onto an infinitely long-lived, zero-width Floquet resonance. Such a resonance is obtained for a frequency-dependent critical field intensity specific to each field-free initial vibrational state. This mechanism, illustrated here for the photodissociation of H_2^+ under a $\lambda=400$ nm intense laser pulse, opens the way to a control scenario of a selective preparation of a given vibrational level that could be used in the context of molecular cooling.

DOI: 10.1103/PhysRevA.77.043413 PACS number(s): 33.80.Gj, 42.50.Hz, 31.15.xg

I. INTRODUCTION

By applying forces that, in energetic terms, are comparable to electron binding energies, intense laser fields can induce unexpected dynamical behaviors in molecules. Thus, while it appears quite natural that the strong radiative interactions would generally facilitate molecular fragmentation, a stabilization of the laser-driven molecular system with respect to its fragmentation has been shown to occur under certain conditions. The underlying mechanism of this strong field stabilization depends on the frequency domain which is addressed.

In the ultraviolet-visible (uv-vis) spectral range (with wavelengths lying within 10 nm to 750 nm), the photon energy (a few electron-volts) is resonant with an electronic transition at finite internuclear distances. The theory of above-threshold dissociation (ATD) [1] and its experimental confirmation [2] then provides a satisfactory understanding of the excitation steps involved in the photofragmentation process: While a single photon brings enough energy for the dissociation to occur, the high intensity of the field may cause the molecule to absorb further photons to go above its dissociation threshold. Important cycle-averaged modifications are then induced in the molecular force field. These modifications first result into the weakening of some chemical bond, by an effect called barrier suppression or bond-softening effect (BS) [2,3]. But by the same token, the modified molecular force field may also lead to the stabilization of the molecule with respect to its dissociation by a mechanism known as the bond-hardening or vibrational trapping (VT) mechanism [4–6]. The interplay between these two complementary mechanisms leads to control scenarios which may be exploited to favor a given reaction pathway or produce velocity and angular selected photofragments [7].

In the infrared (ir) spectral region (with wavelengths ranging from 750 nm to 10^6 nm), a single photon is not energetic enough to induce dissociation and the molecular breakup requires a multiphoton process. In contrast to a uv-vis light, the ir field frequency is of the same order of magnitude as the molecular vibrational frequencies, so that the molecule follows the optical cycle oscillations of the electromagnetic field. In this ir spectral range, the counterpart of VT mechanism is then the dynamical dissociation quenching (DDQ) mechanism [8], which relies on a proper synchronization of molecular wave packets with the fluctuations in time of adiabatic potential energy curves (PECs) which result from the instant distortion of the molecular force field by the laser. Whenever the synchronization ensures a good, almost total, reflection of the vibrational wave packets on a potential energy barrier that is closing as the field is attaining its zero amplitude within the optical cycle, an efficient stabilization is obtained. The DDQ mechanism has recently received an experimental confirmation [9].

One can bring together, within a single laser pulse, these two basic mechanisms (VT and DDQ) which were operating at different frequency ranges (uv-vis and ir, respectively), in a cooperative manner such as to enhance molecular stabilization. We show how this can be done in Ref. [10], by considering the synchronization of the vibrational motion, not with the carrier-wave oscillations, which were chosen in the uv-vis range, but with a pulse envelope that is periodically modulated on a time scale corresponding to an ir frequency. It is then the absolute phase and the modulation frequency of the envelope which play a central role in this synchronization. The relevant force field then consists of adiabatic photon-dressed potentials in the Floquet scheme defined by the uv-vis carrier-wave frequency, with a "breathing" gap at the one-photon avoided crossing, as this gap is modulated in time by the pulse envelope.

Among the new observations made in Ref. [10] on the photodissocation of H_2^+, we noted an enhancement of the VT

*osman.atabek@u-psud.fr
†Also at UFR de Physique Fondamentale et Appliquée, Université Pierre et Marie Curie, 75321 Paris, France; roland.lefebvre@u-psud.fr
‡Also at Laboratoire de Photophysique Moléculaire du CNRS, Univ. Paris-Sud, Bâtiment 210, Campus d'Orsay 91405, Orsay, France; catherine.lefebvre@chm.ulaval.ca
§tung@chm.ulaval.ca

effect that suggested a mechanism involving an adiabatic transport of high-energy field-free vibrational states onto some particularly long-lived Floquet resonances supported by the VT channel. It was suggested that this further stabilization arises when an energy coincidence between the initial vibrational level and the resonance position is encountered, a fact well known in adiabatic-diabatic dynamics [11]. A recent work [12] establishes indeed the existence of such instances and shows that they can even lead to the formation of resonances that are stabilized to the extent of becoming bound states embedded in the continuum (BICs), or zero-width resonances (ZWRs). Such circumstances have already been described in the literature in the context of predissociation [13] or of two interacting resonances [14]. What is the role of these ZWRs in the laser-driven photodissociation dynamics of a generic molecule? Can they be exploited in control problems? The present paper addresses these questions. We start in Sec. II A with the description of the typical molecule+field model system we are considering in our computations. It gives a time-dependent two-state problem of the same form as previously considered for the H_2^+ system, although the intent is to represent a generic situation where the laser field essentially couples a bound electronic state (of some molecule) to a repulsive one, to yield a laser-dressed scheme exhibiting, at the one-photon avoided crossing of these states, BS-like and VT-like adiabatic channels. The birth of ZWRs as the field intensity is varied is unveiled in time-independent calculations of multichannel eigenstates of the Floquet Hamiltonian. Time-dependent two-channel wave-packet calculations, corresponding to solving directly the time-dependent Schrödinger equation for the model laser-driven system, can be interpreted by these resonances to discuss how they are encountered and how they affect the dissociation yield as the dynamics actually unfolds in time. The detailed methodology for the two types of calculations is presented in Secs. II B and II C, while Sec. II D classifies the Floquet resonances. Section III presents and discusses the results of these calculations, with a particular emphasis placed upon the laser conditions to encounter a ZWR, in correlation with a specific field-free vibrational state, and upon the dynamical effect of such an encounter. We discuss in Sec. III C the role that ZWRs may play in vibrational control problems, in particular in vibrational purification processes, with a possible application to laser cooling. We finally address in Sec. III D questions that may arise from the limitations that were initially imposed on the molecular models to simplify the computational workload. These include the restriction to a rotating wave approximation (RWA), the consideration of a one-dimensional, hence rotationless model, and the omission of possibly strong permanent dipole effects. The results obtained by including further channels, either by going beyond the RWA or by taking into account rotational-state couplings, indicate that the existence of ZWRs is a universal concept, and that a control scheme based on them is generic.

II. MODEL AND METHODOLOGY

A. Model

The diatomic molecular system, represented by a one-dimensional model, has two electronic states. The states $|1\rangle$ and $|2\rangle$, taken within the Born-Oppenheimer approximation, have energies $V_{1,(2)}(R)$ and transition dipole moment $\mu_{12}(R)$, function of the nuclear geometry R. $V_2(R)$ is supposed to be purely dissociative, whereas $V_1(R)$ may support discrete levels in addition to a dissociative continuum. With the restrictions to a one-dimensional, two-state model without permanent dipoles (in each electronic state) that we are adopting for now, the following considerations, in particular those concerning the concept of laser-induced ZWRs to be found in Sec. III, are directly applicable to a rotationless homonuclear diatomic system. We will discuss in Sec. III D how these resonances will behave as we relax these restrictions and consider more general situations. The field-induced dynamics is described by the complete time-dependent state, including nuclear motion,

$$|\Psi(R,t)\rangle = \chi_1(R,t)|1\rangle + \chi_2(R,t)|2\rangle. \tag{1}$$

The nuclear wave functions, $\chi_1(R,t)$, $\chi_2(R,t)$, are governed by the time-dependent Schrödinger equation (TDSE), written in the length gauge as

$$i\hbar\frac{\partial}{\partial t}\begin{pmatrix}\chi_1(R,t)\\ \chi_2(R,t)\end{pmatrix} = \left\{T_N + \begin{pmatrix}V_1(R) & 0\\ 0 & V_2(R)\end{pmatrix} - \mu_{12}(R)\mathcal{E}(t)\begin{pmatrix}0 & 1\\ 1 & 0\end{pmatrix}\right\}\begin{pmatrix}\chi_1(R,t)\\ \chi_2(R,t)\end{pmatrix}, \tag{2}$$

where T_N is the nuclear kinetic energy operator, $\mu_{12}=\mu_{21}$ the transition dipole and $\mathcal{E}(t)$ the laser electric field amplitude. This consists of a carrier wave of frequency ω (wavelength λ), lying in the uv-vis spectral range, modulated by a pulse envelope with a frequency Ω lying in the ir range,

$$\mathcal{E}(t) = \begin{cases}\mathcal{E}_0 \sin \Omega t \cos \omega t & \text{for } 0 \le t \le \pi/\Omega,\\ 0 & \text{for } t > \pi/\Omega.\end{cases} \tag{3}$$

Two forms of solutions to the nuclear TDSE [Eq. (2)] will be considered and discussed in the following: Time-dependent wave packets are direct solutions of the TDSE in time domain, starting from some initial wave function; quasistationary or Floquet solutions are frequency-domain representations of periodic, or quasiperiodic, solutions to the TDSE. Results of wave-packet propagations will be analyzed in terms of Floquet resonance states, and emphasis will be placed on certain types of Floquet resonances. It is thus useful to review briefly the basic concepts of Floquet theory as applied to the present model.

The time dependence of the laser field $\mathcal{E}(t)$ as given by Eq. (3) is characterized by two time scales: Fast oscillations of the uv-vis carrier wave occur at the frequency ω; they are modulated by an envelope that involves a much lower frequency Ω. Within some time interval $[\bar{t}-\Delta t, \bar{t}+\Delta t], \Delta t = T_{ir}/N, T_{ir}=2\pi/\Omega$ around $\bar{t}$, with N large enough so that the variations of the pulse envelope over $2\Delta t$ can be neglected, but still ensuring that some oscillations of the high-frequency wave do occur during that time interval, the laser field $\mathcal{E}(t)$ can be considered of constant amplitude, i.e., it can be written $\mathcal{E}(t)=\bar{\mathcal{E}}_0 \cos \omega t$, with $\bar{\mathcal{E}}_0 := \mathcal{E}_0 \sin \Omega \bar{t}$. Without the amplitude modulation, the dynamics under the uv-vis field is well captured by the Floquet representation. Since the amplitude

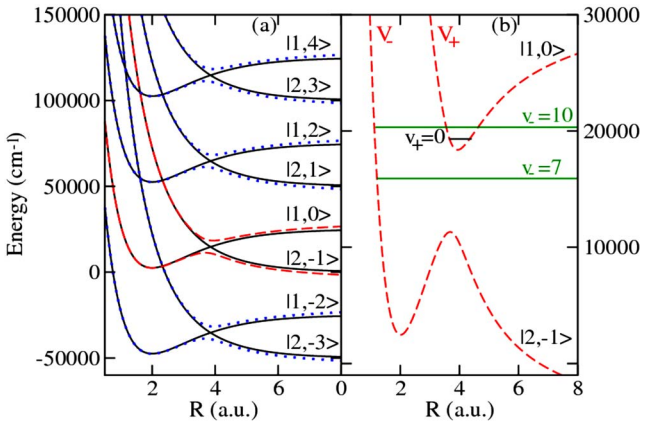

FIG. 1. (Color online) (a) Diabatic (black solid line) and adiabatic (blue dotted and red dashed line) dressed potentials of H_2^+ as a function of the internuclear distance R with their asymptotic channel labels. The adiabatic potentials $V_{\pm}$ at the one-photon crossing (red dashed line) are highlighted in panel (b), together with two shape resonances $v_-=7,10$ and a Feshbach resonance $v_+=0$.

modulation is slow, the Floquet ansatz can still be applied to Eq. (2) with this locally periodic field, albeit approximately, and consists of writing [15]

$$\begin{pmatrix} \chi_1(R,t) \\ \chi_2(R,t) \end{pmatrix} = e^{-iEt/\hbar} \begin{pmatrix} \phi_1(R,t) \\ \phi_2(R,t) \end{pmatrix}, \quad t \in [\bar{t}-\Delta t, \bar{t}+\Delta t], \quad (4)$$

with $\phi_k(Rt)$, $(k=1,2)$, time-periodic functions (over $[\bar{t}-\Delta t, \bar{t}+\Delta t]$ of course). They can thus be Fourier expanded as

$$\phi_k(R,t) = \sum_{n=-\infty}^{+\infty} e^{in\omega t} \psi_{k,n}(R), \quad (5)$$

so that, substituting this Floquet form, Eq. (4), together with Eq. (5) into the TDSE, Eq. (2), one gets, after time integration over an optical cycle, an infinite set of coupled equations for the nuclear wave function Floquet components $\psi_{k,n}(R), k=1,2$,

$$\begin{aligned} &[T_N + V_1(R) + n\hbar\omega - E]\psi_{1,n}(R) \\ &\quad = 1/2\bar{\mathcal{E}}_0 \mu_{12}(R)[\psi_{2,n-1}(R) + \psi_{2,n+1}], \\ &[T_N + V_2(R) + n\hbar\omega - E]\psi_{2,n}(R) \\ &\quad = 1/2\bar{\mathcal{E}}_0 \mu_{21}(R)[\psi_{1,n-1}(R) + \psi_{1,n+1}]. \end{aligned} \quad (6)$$

The structure of these equations is such as to define a parity selection rule: Once a parity of the Fourier indices ("number of photons") n associated with the state $|1\rangle$ is chosen, the nuclear amplitudes $\psi_{1,n}$ supported by this state, dressed by "n photons," [i.e., $V_1(R)+n\hbar\omega$], are coupled only to the amplitudes $\psi_{2,n'}$, supported by the state $|2\rangle$ with a number n' of opposite parity. A typical illustration of the photon-dressed potentials (solid lines) is given in Fig. 1(a), with only four Floquet blocks retained. The reference block corresponds to a single ω-photon absorption described by the crossing of two potentials curves, $V_1(R)+\hbar\omega$ and $V_2(R)$. The two "dressed" electronic states of this block are labeled by two indices, the first denoting the molecular electronic state (1 or 2) and the second the number of photons exchanged with the field (0 for no photon exchange, −1 for the absorption of one photon from the field). The additional blocks correspond to multiphoton processes (−2 and −3 for two- and three-photon absorptions; +1 to +4 for one- through four-photon emissions). The diagonalization of the radiative couplings between the dressed potentials leads to the dressed adiabatic representation, characterized by avoided curve crossings [1,15] [represented by the dotted lines of Fig. 1(a)], and residual nonadiabatic interactions.

As announced above, we have performed two types of calculations to obtain the direct, time-dependent wave-packet solutions of the TDSE [Eq. (2)] on one hand, and its quasistationary Floquet solutions on the other hand.

B. Time-dependent methodology

Starting with an initial state of the form

$$|\Psi(R,t=0)\rangle = \langle R|\chi_1^{(v)}(t=0)\rangle|1\rangle = \langle R|v\rangle|1\rangle, \quad (7)$$

where $|v\rangle$ is one of the discrete vibrational states associated with the electronic state $|1\rangle$ and $|\chi_1^{(v)}(t=0)\rangle = |v\rangle$, we propagate nuclear wave packets by solving Eq. (2) following a procedure thoroughly documented in previous works [15]: For the inner part of the nuclear wave functions defined over the region of the potentials where Hellmann-Feynman forces are nonzero, numerical propagation on a grid uses the standard third-order split-operator algorithm [16], while for the outer part of the wave functions, defined over the asymptotic region of the potential energy curves where these level off each to a constant value, an analytical propagation can be made. If the transition dipole moment behaves as a linear function of R, then this analytical propagation is done by projecting the asymptotic nuclear wave functions onto Volkov-type states [17,18]. The wave-packet propagation is restricted to a time interval $[0, t_f = T_{\rm ir}/2]$.

The observable of interest here is the survival probability, i.e., the probability for the system to remain bound at the end of the pulse, is

$$P_b(v;t_f) = \sum_{v'} p_b(v,v';t_f), \quad (8)$$

where

$$p_b(v,v';t_f) = \frac{|\langle v'|\chi_1^{(v)}(t_f)\rangle|^2}{|\langle \chi_1^{(v)}(t_f)|\chi_1^{(v)}(t_f)\rangle|^2 + |\langle \chi_2(t_f)|\chi_2(t_f)\rangle|^2}, \quad (9)$$

the sum being taken over all the discrete vibrational levels v' of state $|1\rangle$. Note that $P_b(v;t_f)$ actually represents the total bound state population at any time exceeding t_f, since no further decay is possible after t_f. Also, in general, the molecular initial state will be a coherent (pure state case) or incoherent (ensemble case) sum of vibrational states v, rather than being just one of these as considered here. Nevertheless, what we obtain here as $P_b(v;t_f)$ should be useful either to reconstruct the result for any initial state of the molecular system, or to serve as a basis for a specific control scenario concerning a particular v. The understanding we wish to reach is how the dissociation dynamics is unraveled in terms of individual laser-induced resonances.

C. Determination of Floquet resonances

In the Floquet representation, the field-free bound vibrational levels of the electronic state $|1\rangle$, labeled by v, become multichannel Floquet resonances which are exact solutions of Eqs. (6) with appropriate boundary conditions. The calculations of these complex energy resonance wave functions is here conducted by solving the close-coupled equations (6), with Siegert-type boundary conditions (the wave function vanishes in all channels at the origin $R=0$, whereas it satisfies outgoing-wave boundary condition at large R) [19]. These solutions are obtained by the Fox-Goodwin-Numerov shooting-matching procedure on a spatial grid with complex rotation of the coordinate R. This procedure leads to highly accurate, converged results for a broad range of long- to short-lived multichannel resonances, provided the grid characteristics (position of the matching point, complex coordinate rotation angle, step size) are well chosen [20,21]. In practice, the numerical calculations are made with Eqs. (6) truncated to a finite number N of Floquet blocks, i.e., to $2N$ channels, and we will refer to the calculated Floquet states as $2N$-channel resonances. For a given (local) field intensity $I=\bar{\mathcal{E}}_0^2$, the Floquet resonances are labeled by the quantum number v, in reference to their field-free counterpart. Their complex energies are denoted as $E_v-i\Gamma_v/2$. As the laser intensity is lowered to vanishing value, $E_v-i\Gamma_v/2$ tends to the real energy of the corresponding discrete vibrational level v of the photon-dressed potential $V_1(R)+\hbar\omega$.

For a purely time-adiabatic pulse shape, Floquet resonances are parametrized by the time $\bar{t}$ through the field amplitude $\bar{\mathcal{E}}_0:=\mathcal{E}_0 \sin \Omega\bar{t}$. As mentioned above, their time-dependent complex energies $E_v(\bar{t})-i\Gamma_v(\bar{t})/2$, are such that $E_v(0)$ reduces to the field-free vibrational energy E_v, and $\Gamma_v(0)=0$. The probability for the system to remain bound, while it adiabatically evolves as a pure Floquet resonance v under the pulse can then be calculated as

$$P_b(v;t_f)=\exp\left(-\int_o^{t_f}\Gamma_v(t')dt'\right). \tag{10}$$

The possibility of considering Eq. (10) as a valid approximation for a full time-dependent wave-packet evolution model [Eq. (8)] rests on the assumption of an adiabatic transport of Floquet states, assumption which will constitute the subject matter of the discussions in the following sections.

D. Floquet resonance classification

Just to define a simple classification scheme of the Floquet resonances, we will consider two simplifications. First, focusing on single photon processes, we would restrict the coupled equations (6) to a single Floquet block, as illustrated in Fig. 1(b). Second, going to the dressed adiabatic representation, we would omit, in a zeroth-order approximation, the residual nonadiabatic couplings between the adiabatic potentials $V_+(R)$ and $V_-(R)$. The stronger the field intensity is, the better this last approximation would be. On the other hand, we will also need to assume that the field intensities involved are weak enough to allow for a single photon description.

By referring to this simplified scheme, Floquet resonances can be said to belong to one of the two following categories, depending on the adiabatic potential they are associated with and within the limit of the intermediate field intensity range we just delineated. Actually, we do recalculate the resonances using the same Fox-Goodwin-Numerov algorithm within this single-block dressed adiabatic Floquet approximation and, by comparing them with the multichannel resonances, we can check the validity of this classification. The resonances that are accommodated by the lower adiabatic potential $V_-(R)$ are of shape type [22], whereas those belonging to zeroth order to the upper adiabatic potential $V_+(R)$ are of Feshbach type [22]. The shape resonances are labeled by v_-, their complex energies being $E_{v_-}-i\Gamma_{v_-}/2$. These can in turn be distinguished either as long-lived tunnel resonances (the lowest-energy ones), which are well protected against dissociation by the field-induced potential barrier, or as short-lived above-the-barrier resonances. The field strength dependence of the lifetimes is accounted for by the BS mechanism. The stronger the field is, the lower the potential barrier will be, leading to shorter lifetimes. Two typical examples of short-lived shape resonances are illustrated in Fig. 1(b): one, the $v_-=7$ level, at low energies, and one at higher energies, the $v_-=10$ level. As for the Feshbach resonances, they are in principle long lived. Their behavior with respect to the field strength is opposite to that of the shape resonances: The stronger the field is, the lower will the residual nonadiabatic couplings be, resulting in a more efficient VT mechanism. Moreover, within the single-block uncoupled adiabatic assumption defined above, the Feshbach resonances are nothing else than (at zeroth-order approximation), the discrete bound states v_+ of the V_+ potential, with real energies E_{v_+}. The position of $v_+=0$ is given as an example in Fig. 1(b).

III. RESULTS AND DISCUSSION

Both types of calculations (time-dependent wave-packet propagation and time-independent, or rather, time-parametrized Floquet resonance determination) were made for a one-dimensional representation of H_2^+ taken as an illustrative example. The two electronic states are then identified as the ground state $|1\rangle\equiv|g\rangle=|^2\Sigma_g^+\rangle$ and the first excited state $|2\rangle\equiv|u\rangle=|^2\Sigma_u^+\rangle$ of the molecular ion. The potentials $V_{g(u)}(R)$, as well as the transition dipole moment $\mu_{gu}(R)$ are taken from [23]. It is precisely these potentials, dressed by a uv-vis ($\lambda=400$ nm, $\omega=0.1139$ a.u.) photon, which are displayed in Fig. 1. The laser peak intensity is $I_{\max}=1.2\times10^{13}$ W/cm^2 (0.0003 a.u.) which corresponds to $\mathcal{E}_0=I_{\max}^{1/2}=9.494\times10^9$ V/m [in Eq. (3)], whereas the pulse shape is characterized by $\Omega=635$ cm^{-1} (0.0029 a.u.). The electronic ground manifold accommodates 19 vibrational levels ($|v\rangle, v=0-18$), that would, in principle, lead to 19 Floquet resonances when the laser field is switched on, resulting from the interplay of all the potential channels displayed in Fig. 1. Calculations of multichannel Floquet resonances were made by keeping four Floquet blocks, i.e., eight channels, to ensure convergence of resonance properties, i.e., field-induced Stark shifts and widths (with four significant figures accuracy), for the whole range of instantaneous intensities covered by the laser pulse.

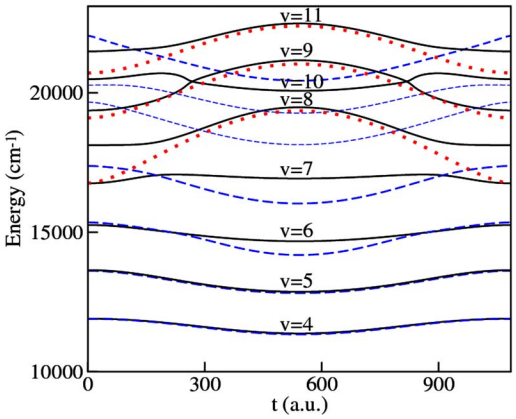

FIG. 2. (Color online) Trajectories, as a function of the pulse time, of the real part of the energies E_v of the Floquet resonances (black solid line) for $v=4-11$, of the real part of the energies E_{v_-} of the shape resonances of the lower adiabatic potential (blue dashed line) and of the eigenvalues E_{v_+} of the upper adiabatic potential (red dotted line) at the one-photon crossing.

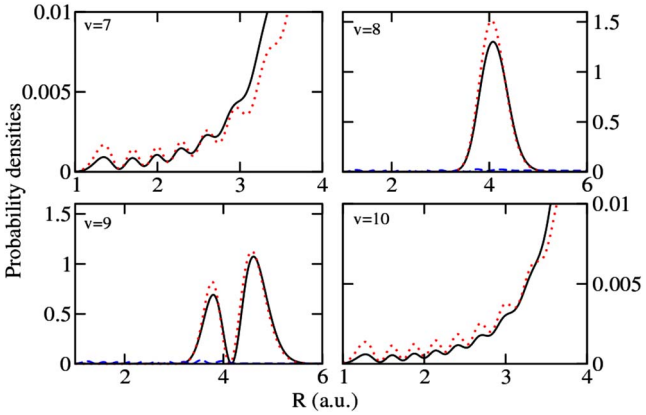

FIG. 3. (Color online) Probability densities as a function of R for $v=7,8,9,10$. Solid black lines are for the Floquet resonances, red dotted lines are for the corresponding shape ($v=7$ and 10) or Feshbach ($v=8$ and 9) resonances accommodated, respectively, by the adiabatic potential V_- and V_+ of the reference Floquet block. The blue dashed lines represent the sum of the probabilities on all the other channels.

A. Adiabatic transport

The most critical point when comparing the bound probabilities calculated through Eq. (8), using the direct solutions of the TDSE, and through Eq. (10), using a time-parametrized Floquet resonance's width, is the question of adiabaticity in the Floquet dynamics. This adiabaticity implies that a field-free initial v-state population is continuously transported onto a single Floquet resonance v during the pulse rise and evolves according to this Floquet resonance characterized by a time-parametrized dissociation rate $\Gamma_v(t)$. During the fall of the pulse, the population transfer occurs from the Floquet resonance v back to the initial vibrational state. There is thus no population loss of the initial vibrational population, except for the continuous decay of the single active Floquet resonance, which is precisely accounted for by Eq. (10). Figure 2 illustrates the dynamical behavior of a series of Floquet resonances calculated by solving the close-coupled equations (6), within the total duration of the laser pulse [i.e., for $t=0$ to 1086 a.u. (26 fs)]; only the resonances' positions, i.e., the real part of their energies, are shown as a function of time. The "trajectories" of these energies are symmetric with respect to the mid-pulse time [$t=543$ a.u.(13 fs)] reflecting the symmetric intensity distribution of the pulse shape. At $t=0$ and $t=1086$ a.u. one recovers the eigenenergies of the field-free initial vibrational states, ($v=4-11$), of the ground electronic potential $V_g(R)$. On the same figure, we also show the variations of single-channel resonance energies defined by the dressed adiabatic, single-Floquet-block, potentials. More precisely, we exhibit the eigenenergies (E_{v_+}) of levels supported by the upper, closed, adiabatic potential $V_+(R)$ (red dotted lines) as well as the real part of the eigenenergies (E_{v_-}) of the shape resonances accommodated by the lower open adiabatic potential $V_-(R)$ (blue dashed lines). The aforementioned two classes of Floquet resonances can clearly be identified. Floquet resonances up to $v\leq 7$ follow trajectories similar to those of the shape resonances. Higher energy Floquet resonances follow closely the energies E_{v_+} of the bound states supported by $V_+(R)$ (which are zeroth-order approximations to Feshbach resonances). This is in particular the case for $v=8,9,11$. Although the $v=10$ Floquet resonance lies in the same energy range, it does not follow the trajectory of a discrete level of $V_+(R)$; it appears rather to belong to the first class of resonances, and is more appropriately qualified as an above-the-barrier shape resonance. This can be understood by invoking a density-of-states argument: There is only a limited small number of eigenstates of $V_+(R)$ and they cannot account for all the Floquet resonances within a given energy window. We now focus on four typical Floquet resonances, namely, the $v=7$ and 10 states, representing the class of shape-type resonances and the $v=8$ and 9 states, illustrating the class of Feshbach-type resonances. That the dressed adiabatic representation effectively captures the effect of the radiative couplings, within and between the Floquet blocks, can directly be judged by looking at probability densities associated with the multichannel wave function of the Floquet resonances [defined by Eq. (5) with four Floquet blocks], and by comparing them to the ones of the corresponding shape or Feshbach resonance wave functions. This is shown in Fig. 3 with all resonance wave functions calculated at the mid-pulse, peak intensity. The solid (black) line gives, as a function of the internuclear distance, the probability density of the Floquet resonances. As expected, the $v=7$ Floquet resonance which, on energetic grounds, cannot be trapped on the upper adiabatic potential, shows a fast decay (i.e., a large escaping population), as seen through the large values of the densities at large distances R. A completely different situation prevails for $v=8$ and 9 with densities well localized at short internuclear distances, precisely around the avoided crossing, $R_c \approx 4$ a.u., indicating that they are vibrationally trapped. In contrast, the $v=10$ Floquet resonance which energetically lies above the bottom of the upper adiabatic potential $V_+(R)$, is not trapped. We can actually make a more accurate identification of these multichannel Floquet resonances by plot-

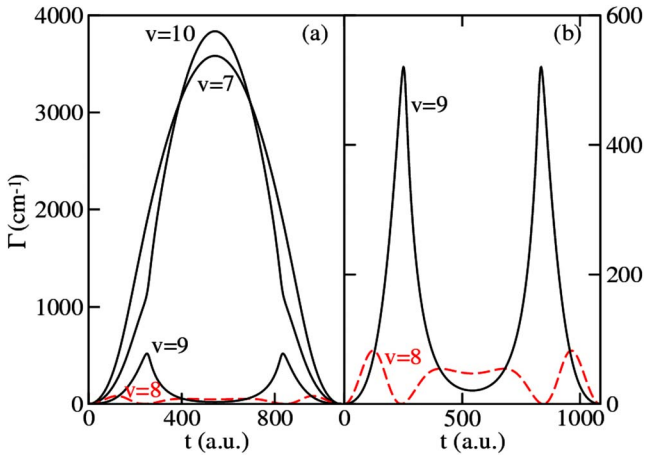

FIG. 4. (Color online) (a) Rate Γ of Floquet resonances as function of the pulse time for $v=7-10$. Panel (b) is an enlargement for $v=8$ (dashed red line) and $v=9$ (solid black line)

ting on the same graphs the probability densities of the single-channel dressed adiabatic shape and Feshbach resonances. These are shown by the dotted (red) line. For $v=8$ and 9, a quasiquantitative comparison can be made between the Floquet and the corresponding Feshbach resonance wave functions, beyond the similarity in their nodal structures (i.e., one finds 0 and 1 node in the $v=8$ and 9 resonances, as in the $v_+=0$ and $v_+=1$ states, respectively). This clearly shows that the Floquet resonances $v=8$ and 9 are, at the peak intensity of the pulse, very close to the $v_+=0$ and $v_+=1$ Feshbach resonances. A somewhat similar conclusion holds for the $v=7$ and 10 Floquet resonances, but now the corresponding single-channel resonances are shape resonances. The quality of the agreement, between the $v=7$ and 10 multichannel Floquet wave functions and the corresponding single-channel shape-resonance wave functions, can be judged through the oscillatory structures and the increasing wings found at $R>3$ a.u. in the densities shown in the corresponding panels of Fig. 3.

B. Zero-width resonances

The most important information, in so far as the dissociation dynamics is concerned, is the width of the multichannel Floquet resonances for the field intensities covered by the laser pulse. Figure 4(a) collects, for $v=7-10$, the behaviors of the corresponding widths Γ_v as a function of time. Here again the difference between the two classes of resonances is clearly marked. The Floquet resonances $v=7$ and 10, identified above to be of the shape-resonance type, show large widths, that can go up to 4000 cm^{-1} at mid-pulse (i.e., at peak intensity). These are broad, fast-decaying resonances. They are to be contrasted with the long-lived Feshbach-type Floquet resonances $v=8$ and 9, whose widths do not exceed 500 cm^{-1} for the range of intensity covered by the full pulse shape. Figure 4(b) shows an enlargement of the curves for $v=8$ and $v=9$. It points to an important and astonishing observation specific to $v=8$. At $t=244$ a.u. (corresponding to a critical intensity $I_c=4.996\times10^{12}$ W/cm^2), $\Gamma_{v=8}$ vanishes completely, i.e., it is strictly zero. This is a very peculiar situation of a zero-width resonance [12], where for a particular field intensity, a Feshbach-type resonance becomes (very accurately) an infinite-lived discrete bound state. Such resonances have already been discussed in the literature in terms of real poles of the scattering amplitude as BICs [14]. The critical intensity can be numerically derived, within arbitrary accuracy, leading to values of Γ_v of the order of 10^{-10} cm^{-1}, in a numerically converged and robust scheme. It is worthwhile noting that there is also a critical intensity for the Floquet resonance $v=9$, which is precisely $I_c=1.694\times10^{13}$ W/cm^2. This intensity, being higher than the peak intensity of the pulse under consideration presently, is simply not reached in this case, and hence the transformation of the $v=9$ resonance into a BIC is not observed with the present pulse, and $\Gamma_{v=9}$ remains finite at all times. An interpretation can be given, of the appearance of ZWRs at critical intensities, within a semiclassical approach, in terms of a destructive interference between different components of the semiclassical resonance wave function; these are governed by diabatic and adiabatic phase factors associated with $V_\pm(R)$ [11] of the single-block adiabatic representation, and their interplay is best expressed by referring to Child's diagrammatic method [24]. Very sharp resonances are obtained, regardless of the value of the coupling parameter, provided that the energy of a vibrational level $\tilde{v}$ of a "modified" (see below for more precisions) ground diabatic potential is close to a "modified" vibrational level $\tilde{v}_+$ of the adiabatic potential $V_+(R)$. More precisely, an approximate expression for the resulting resonance width is [25]

$$\Gamma=\frac{2\pi}{\hbar}\frac{e^{2\pi\nu}(e^{2\pi\nu}-1)\omega\omega_+}{[\omega_++(e^{2\pi\nu}-1)\omega]^3}(E_{\tilde{v}}-E_{\tilde{v}_+})^2, \tag{11}$$

where ω and ω_+ are local energy spacing's of the modified diabatic and adiabatic potentials. ν is the coupling parameter, that, in a Landau-Zener type of approximation, is given by

$$\nu=\frac{\mu_{gu}^2(R_c)I}{\hbar\bar{v}|\Delta F|}, \tag{12}$$

$\bar{v}$ and ΔF being the classical velocity and difference of slopes of the diabatic potentials at the diabatic crossing point R_c. The "modification" affecting the ground diabatic potential is indicated in Fig. 5(b). Actually, this is a piecewise potential based on two adiabatic curves: $V_-(R)$ for $R<R_c$, $V_+(R)$ for $R>R_c$, with a discontinuity at $R=R_c$. It is worthwhile noting that for low field strengths, the so-called "modified" diabatic potential is close to the original diabatic ground-state potential $V_g(R)$. The energies $E_{\tilde{v}}$ and $E_{\tilde{v}_+}$ are obtained from semiclassical quantization conditions involving energy-dependent phase factors,

$$\alpha_\pm=\int_{a_\pm}^{R_c}k_\pm(R)dR,\quad \beta_+=\int_{R_c}^{b_+}k_+(R)dR, \tag{13}$$

$k_\pm(R)$, being the wave numbers associated with $V_\pm(R)$, $\{k_\pm^2(R)=\frac{2m}{\hbar^2}[E-V_\pm(R)]\}$, and $a_\pm, b_+$, the left and right turning points. Specifically, $E_{\tilde{v}}$ is obtained by the quantization condition

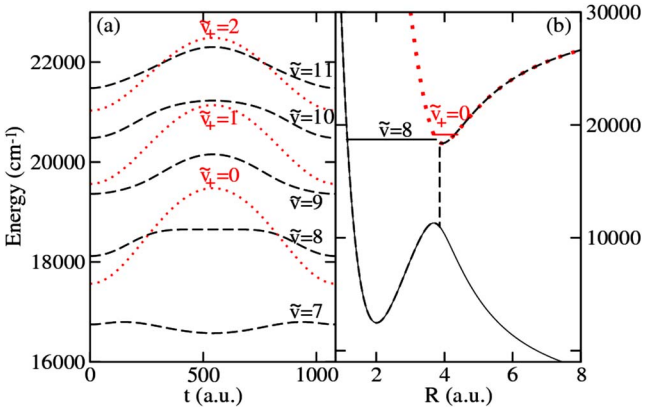

FIG. 5. (Color online) (a) Trajectories as a function of the pulse time of the modified diabatic energies of levels $\tilde{v}=7,8,9,10,11$ (dashed black line) and those of the modified adiabatic levels $\tilde{v}_+=0,1,2$ (red dotted line). (b) Modified diabatic potential (dashed black line) together with the upper (red dotted line) and lower (thin black line) adiabatic potential. Semiclassical energy levels $\tilde{v}=8$ and $\tilde{v}_+=0$ are in a quasicoincidence situation.

$$\alpha_- + \beta_+ = (\tilde{v} + 1/2)\pi. \tag{14}$$

As for $E_{\tilde{v}_+}$, the quantization condition must be modified to include an additional energy-dependent phase factor χ,

$$\alpha_+ + \beta_+ + \chi = (\tilde{v}_+ + 1/2)\pi, \tag{15}$$

where

$$\chi = \arg \Gamma(i\nu) - \nu \ln \nu + \nu + \pi/4. \tag{16}$$

It can be shown that in the strong coupling case χ is close to zero, whereas for low-field intensities it can be taken, within a good approximation, to be $-\pi/4$. The energies $E_{\tilde{v}}$ and $E_{\tilde{v}_+}$ resulting from an iterative resolution of Eqs. (14) and (15), using a Newton-Raphson algorithm, are plotted against time as a parameter in Fig. 5(a) for levels $\tilde{v}=7-10$ and $\tilde{v}_+=0-2$ (the "modified" counterparts of the v_+ considered above to be in correspondence with the $v=8$ and 9 multichannel resonances). At time $t=244$ a.u., corresponding to a field intensity of $I_c=4.996\times10^{12}$ W/cm^2, the trajectories followed by $E_{\tilde{v}=8}$ and $E_{\tilde{v}_+=0}$ cross each other. This corresponds to a coincidence of the two modified vibrational states $\tilde{v}=8$ and $\tilde{v}_+=0$ [Fig. 5(b) shows a close coincidence situation, found exactly at mid-pulse, i.e., at the peak intensity]. The consequence of this, according to Eq. (11), is precisely to produce a ZWR as has been numerically found in Fig. 4. For the intensities under consideration there are no energy coincidence possible for $\tilde{v}=7,8,9,10$, as these cannot be trapped in any Feshbach resonance. For the case of $\tilde{v}=11$, it turns out that, at a different time $t=405$ a.u., a coincidence with $\tilde{v}_+=2$ occurs, leading again to a ZWR with, however, a different critical intensity $I_c=1.02\times10^{14}$ W/cm^2.

C. Zero-width resonances and control of vibrational motions

How does the existence of ZWRs manifest itself in the actual time-dependent wave-packet dynamics of the laser-driven molecule? What role can they play in control problems? In a previous work [10], we found an indication of a marked selective enhancement of the VT process (which is a form of what we called dynamical dissociation quenching process, specific to the uv-vis spectral range) in H_2^+, under basically the same type of field as considered here, for an initial vibrational state $v=8$. It was conjectured that this enhancement is due to a resonance stabilization at a diabatic-adiabatic energy coincidence. Such a coincidence and its consequence, the encounter of a ZWR, are now well established above with the explicit calculation of the critical intensity I_c for its occurrence, and by checking that I_c lies within the range of the instantaneous intensities covered by the pulse. It remains to compare the total survival probability $P_b(v;t_f)$ as calculated either by wave-packet time-dependent calculations, i.e., by solving the TDSE [Eq. (2)] and using Eq. (8), or by accumulating dynamical Floquet resonance lifetimes according to Eq. (10), assuming time-adiabatic

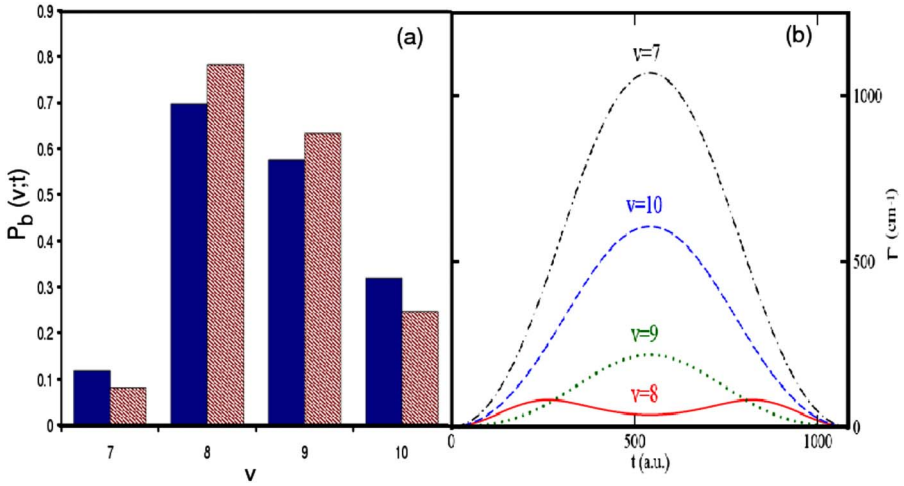

FIG. 6. (Color online) (a) Total survival probabilities $P_b(v;t_f)$ as a function of the initial states $v=7-10$ obtained by a time-dependent calculation [blue, see main text Eq. (8)] and by a time-independent calculation [dashed red, see main text Eq. (10)]. (b) Rate Γ of Floquet resonances as a function of the pulse time, for $v=7-10$. The calculations are done with peak intensity $I=3\times10^{12}$ W/cm^2.

transport of Floquet states. Figure 6(a) gives this comparison for the four initial vibrational states $v=7,8,9,10$ in the form of a histogram, the corresponding widths Γ being plotted against time in panel (b). A qualitative agreement is reached, in so far as the two calculations lead to a survival probability distribution peaked on $v=8$, where $P_b(v;t_f)$ is larger than 0.6. The results of the preceding section show that the particularly large survival probability affecting $v=8$ is due to the fact that a ZWR was approached during the laser pulse duration as shown in Fig. 6(b). The differences, seen in Fig. 6(a), between the results of the complete time-dependent wave-packet propagations and those of the Floquet resonance calculations reflect the degree of deviation from adiabaticity, as found in the actual dynamics. Alternatively, the degree of adiabaticity, and deviations from it, can also be measured by computing the normalized distribution of probability to find the system on a given final vibrational level v', when its wave-packets dynamics starts from an initial level v. This is defined by Eq. (9). Figure 7 gives these distributions for $v=7$ [panel (a)] and 8 [panel (b)] for two field intensities $I=3\times10^{12}$ W/cm^2 and $I=1\times10^{12}$ W/cm^2. Obviously, the most adiabatic pulse (the one corresponding to the lowest intensity) leads to a final probability distribution peaked on the initial vibrational state, i.e., at $v'=v$. Deviations from adiabaticity causes an appreciable population of Floquet resonances that are distinct from the one correlating to the initial v and hence, are characterized by different critical intensities. Returning to Fig. 6(a), the lower survival probability that the actual wave-packet dynamics leads to at the end of the pulse for $v=8$ (when compared with the Floquet resonance adiabatic transport result), reflects this fact: Nonadiabatic transitions to other Floquet resonances, be they small, reduce the population of the $v=8$ resonance, the one which acquires the narrowest width during the pulse.

We now turn to a second illustration of the role of ZWRs in the time-resolved molecular dynamics and of its exploitation in control problems. For this, consider again the H_2^+ model system but this time, subjected to a quasirectangular pulse with a peak intensity favoring the trapping of a specific v, $v=8$ say. The constant central section of the pulse will be preceded and succeeded by rise and fall sections that are sufficiently smooth and slow to ensure the adiabatic transports of Floquet resonances from and to field-free vibrational states. To fix the idea, consider the following pulse:

$$\mathcal{E}(t)=\begin{cases}\mathcal{E}_c \sin \Omega t \cos \omega t & \text{for } 0\le t\le \dfrac{\pi}{2\Omega},\\ \mathcal{E}_c \cos \omega t & \text{for } \dfrac{\pi}{2\Omega}\le t\le \dfrac{\pi}{2\Omega}+\tau,\\ \mathcal{E}_c \sin \Omega(t-\tau)\cos \omega t & \text{for } \dfrac{\pi}{2\Omega}+\tau\le t\le t_f=\dfrac{\pi}{\Omega}+\tau,\end{cases} \tag{17}$$

where $\mathcal{E}_c=(I_c)^{1/2}$, I_c being the critical intensity for $v=8$, ω and Ω being the same as above. In an ideal case, the $v=8$ Floquet resonance is trapped as a ZWR when the pulse enters the plateau region and the resonance width vanishes (this will occur at $t=\pi/2\Omega$), its decay is in principle stopped during the plateau duration τ. This is based on the assumption of an adiabatic transport leading to well separated resonances, which is valid for sufficiently low critical intensities conferring narrow enough widths for neighboring resonances ($v=7,9,10$). For τ sufficiently large, all other Floquet resonances, driven by the same pulse, would have decayed to near complete depletion by the end of the pulse, so that only the $v=8$ resonance would survive and will be, in the case of a full adiabatic transport, transformed back to the $v=8$ vibrational state of the field-free molecule.

To illustrate this strategy, we start from an initial wave packet which is a coherent sum of four field-free vibrational states lying in the neighborhood of $v=8$ state given by

$$|\Psi(R,t=0)\rangle=\sum_{v=7}^{10} c_v\langle R|\chi_1^{(v)}(t=0)\rangle|1\rangle. \tag{18}$$

With equal weight on each state, $c_v^2=1/4$, we aim to show that $v=8$ state is favored under this laser pulse. Figure 8 depicts, for increasing lengths (τ) of the plateau, the residual probabilities $p(v;t_f)$,

$$p(v;t_f)=\frac{|\langle 1|\langle v|\Psi(t_f)\rangle|^2}{\|\Psi(t_f)\|^2} \tag{19}$$

for $v=7,8,9$, and 10. The calculations are done for four peak intensities around the critical one ($I_c=4.996\times10^{12}$ W/cm^2), which actually turns out to be the most efficient for trapping the $v=8$ resonance when increasing τ. One would expect, at the largest value of τ shown ($\tau=5700$ a.u.$=139$ fs), that no population is left on any vibrational level, except on $v=8$. However, nonadiabatic transport, when switching on and off the laser pulse, is responsible for residual population observed on $v=7$; a situation that can be understood from the broad width which $v=7$ resonance acquires at large field intensities and which leads to overlap with $v=8$ resonance. This can be attenuated by increasing adiabaticity, with a lower peak intensities, as obtained with $I=3\times10^{12}$ W/cm^2 for instance. Imagining now an arbitrary initial wave packet, we can see that an adequate combination of pulse plateau duration and intensity will selectively keep the nondissociative population in the $v=8$ vibrational state.

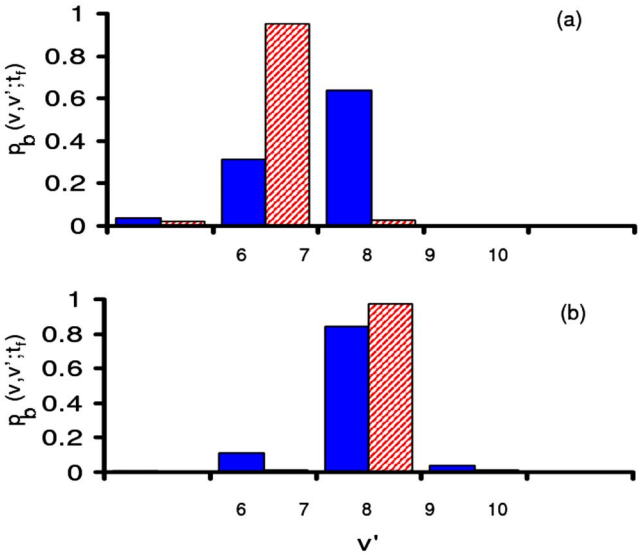

FIG. 7. (Color online) Normalized final probability distributions $p_b(v,v';t_f)$ on different final v' levels for initial states (a) $v=7$ and (b) 8 and for two field peak intensities $I=10^{12}$ W/cm^2 (dashed red) and $I=3\times10^{12}$ W/cm^2 (blue).

The application of this strategy using the critical intensity for $v=8$ would represent a very efficient control scheme for purifying the vibrational content of a molecular state. This is based on the existence of an intensity at which a vibrational state becomes a zero-width Floquet resonance. The critical intensity of a given vibrational state, as obtained from a two-channel Floquet formalism, may be used as a guide to produce an even longer surviving state in the time evolution of the wave packet. It turns out however that this requires a delicate compromise (not solved yet), between the adiabatic attainability of the ZWR and the time that such an adiabatic transport would necessitate. The longer the time is (for a better adiabaticity), the less efficient the process will be, as the dissociation occurs during the preparation of the ZWR. This strategy also relies on an adiabatic switch-on and switch-off of the laser-molecule interactions to ensure the adiabatic, i.e., one-to-one vibrational state/Floquet resonance transformations during the pulse. The selective population control of another vibrational state ($v\neq8$) would necessitate a specific choice of a different photon wavelength involving a different critical intensity. This will induce a reorganization of the dressed scheme and, in particular, a displacement of the one-photon curve-crossing region in such a way to ensure a diabatic-adiabatic coincidence situation near the designated vibrational level, i.e., the existence of a ZWR in this energy range. Decreasing the laser wavelength also opens the possibility of decreasing the critical intensity, a situation which would facilitate the adiabatic attainability of the ZWR. Moreover, the resulting Floquet resonances would be better separated and bear resemblance to their corresponding field-free states. It is then possible to prepare a pure molecular vibrational state (of a given v), when the initial state is a coherent or incoherent superposition of these states. Such a preparation scheme, which is also a vibrational purification, could be extended to obtaining cold molecular species by selectively populating the lowest rovibrational state [26,27]. Research along these lines is actively pursued in our groups.

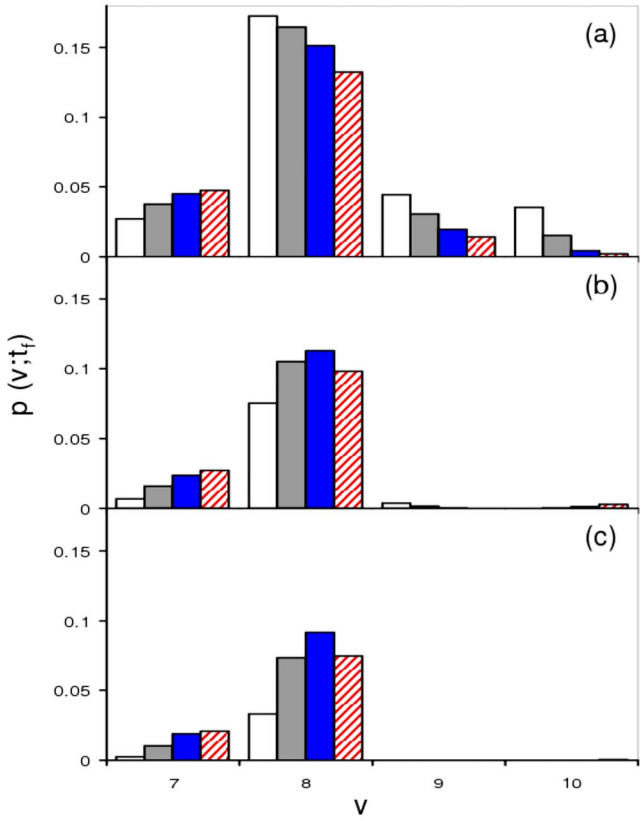

FIG. 8. (Color online) Normalized final residual probability distributions $p(v;t_f)$ on different final v levels for the initial state $|\Psi(R,t=0)\rangle=\Sigma_{v=7}^{10}c_v\langle R|\chi_1^v(t_0)\rangle|1\rangle$, with $c_v^2=1/4$ with the peak intensities $I=3\times10^{12}$ W/cm^2 (white), 4×10^{12} W/cm^2 (gray), 4.996×10^{12} W/cm^2 (blue), and 6×10^{12} W/cm^2 (dashed red) for different pulse shapes with plateau duration (a) $\tau=0$, (b) $\tau=2280$ a.u., and (c) $\tau=5700$ a.u.

D. Robustness of the zero-width resonance concept

Will the zero-width resonances, and the above control scheme based on their exploitation, survive variations in the model potentials? These may arise for instance from nonzero permanent dipole effects or from molecular rotations and/or misalignment. In so far as both of these effects lead to an enrichment of the Floquet scheme by the inclusion of new channels, it suffices to take one of them specifically as an example to assess the above question. Concentrating on the effects of molecular rotations, we have thus extended the time-independent resonance calculations of Sec. II C to include laser-coupled rotational states. This is done by writing the Floquet state as a function of both R and θ, the polar angle of the internuclear axis with respect to the direction of the linearly polarized electric field, considered to be the z axis of the laboratory-fixed coordinate system. Because of cylindrical symmetry, the azimuthal angle, φ, can be separated out and the rotational quantum number M associated with the z component of the molecular rotational angular momentum is conserved. Considering the $M=0$ component,

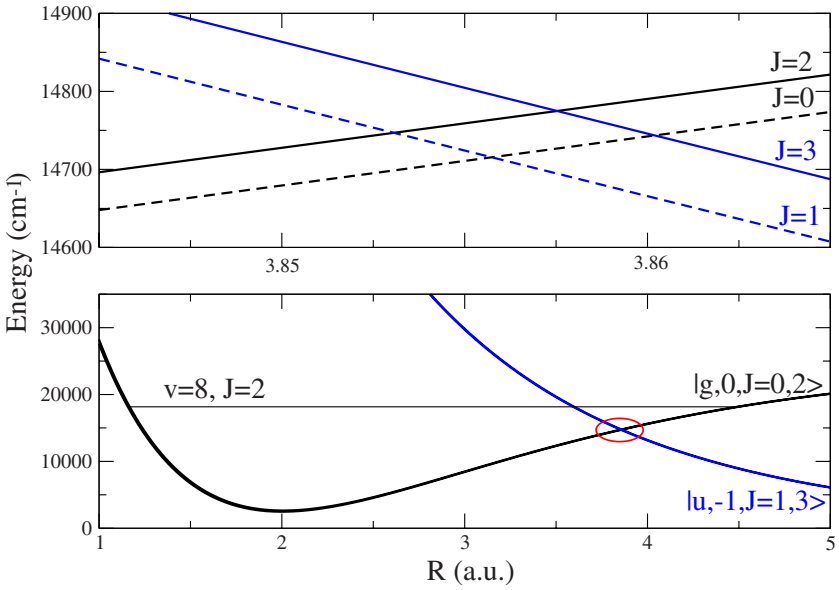

FIG. 9. (Color online) Ground (black line) and excited (blue line) dressed potentials as a function of the internuclear distance R for different rotational quantum numbers $J=0,1,2,3$. The energy of the diabatic level $v=8, J=2$ is indicated by the thin horizontal line. The upper panel is an enlargement of the crossing region (red ellipse of the lower panel).

the g and u components of the Floquet wave function, previously defined in Eq. (5), are now of the form

$$\phi_k^{M=0}(R,\theta,t) = \sum_{n=-\infty}^{+\infty} \sum_{J'} e^{in\omega t} Y_{J',M=0}(\theta)\psi_{k,J'}(R) \quad (k=g,u), \tag{20}$$

where $Y_{J,M}$ denotes the usual spherical harmonics. The coupled equations (6) are then replaced by

$$\left(T_N + V_g(R) + \frac{\hbar^2}{2\mathcal{M}}\frac{J(J+1)}{R^2} + n\hbar\omega - E\right)\psi_{g,n,J}(R)$$
$$= 1/2\bar{\mathcal{E}}_0\mu_{gu}(R)\sum_{J'}\langle Y_{J,M=0}|\cos\theta|Y_{J',M=0}\rangle[\psi_{u,n-1,J'}(R)$$
$$+ \psi_{u,n+1,J'}(R)],$$

$$\left(T_N + V_u(R) + \frac{\hbar^2}{2\mathcal{M}}\frac{J(J+1)}{R^2} + n\hbar\omega - E\right)\psi_{u,n,J}(R)$$
$$= 1/2\bar{\mathcal{E}}_0\mu_{ug}(R)\sum_{J'}\langle Y_{J,M=0}|\cos\theta|Y_{J',M=0}\rangle[\psi_{g,n-1,J'}(R)$$
$$+ \psi_{g,n+1,J'}], \tag{21}$$

where $\mathcal{M}$ is the reduced mass of the nuclei. The angular couplings [28]

$$\langle Y_{J,M=0}|\cos\theta|Y_{J',M=0}\rangle = [(2J+1)(2J'+1)]^{1/2}\begin{pmatrix} J & 1 & J' \\ 0 & 0 & 0 \end{pmatrix}^2 \tag{22}$$

imply the selection rule $J'=J\pm1$ accompanying one-photon ($\Delta n=\pm1$ selection rule) transitions between the two electronic states $|g\rangle$ and $|u\rangle$. In the rotationless, one-dimensional case discussed above, we have already seen that retaining but a single Floquet block, i.e., the two dressed states $\{|g,0\rangle,|u,-1\rangle\}$, corresponding to single photon processes, is sufficient to capture the dynamics; indeed, within the intensity range considered here, the ZWRs are preserved with the inclusion of further Floquet blocks, which has little effect on their appearance or on the values of the critical intensities. We have thus limited our analysis of rotational effects to a single Floquet block.

In addition to the dressing by the relative "photon number" n (which are 0 and −1 in the single Floquet block description), the two electronic states $|g\rangle,|u\rangle$ are further dressed by the rotational quantum number J. We have restricted this to the few values shown in Fig. 9, centered about $J=2$ and accessible from this central value by applying the selection rule $J'=J\pm1$ successively. Thus, the channel $|g,0,J=2\rangle$ is coupled to the $|u,-1,J=3\rangle$ and $|u,-1,J=1\rangle$ channels, the latter being in turn coupled to $|g,0,J=0\rangle$. The upper panel of Fig. 9 shows an enlarged view of the potentials in the region of their field-induced crossings. Figure 10 shows the rate Γ of the Floquet resonance issued from the diabatic level

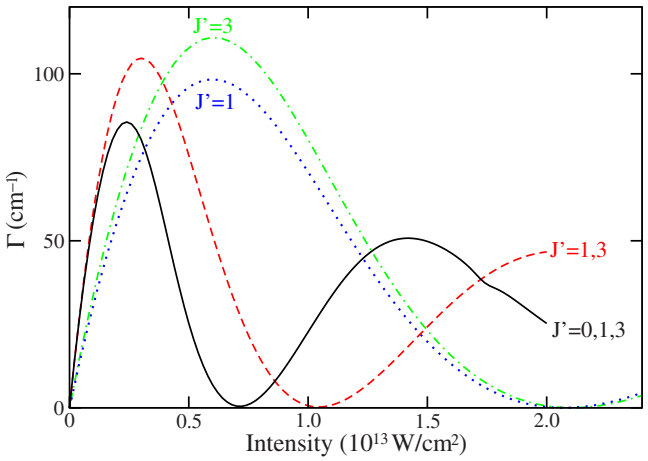

FIG. 10. (Color online) Total dissociation rates of the diabatic state $v=8, J=2$ as a function of the field intensity, with successive inclusions of the rotational states $J'=1$ (dotted blue line), $J'=3$ (dashed-dotted green line), $J'=1,3$ (dashed red line), $J'=0,1,3$ (full black line).

$v=8, J=2$ as a function of field intensity. The rotational quantum number J' shown therein indicates which rotational channels were considered coupled to the reference channel $J=2$. The two curves labeled $J'=1$ and 3 thus correspond to a two-channel calculation; they lead to almost the same critical intensity, $I_c=2.08\times10^{13}$ W/cm^2, for the appearance of a ZWR in the energy region of the $v=8$ state. This critical intensity is about 4 times the one obtained in the rotationless model, which was also limited to two potentials (channels), one closed, one open, of the same forms. This scaling effect is related to the angular couplings in Eq. (21) which, for this case ($J=2, J'=1,3$), take on values close to 0.5. Since the radiative coupling goes as $1/2\sqrt{I}\mu(R)\langle Y_{J,M=0}|\cos\theta|Y_{J',M=0}\rangle$ we need an intensity 4 times larger to produce the same effect as found in the rotationless case. The curves labeled $J'=1,3$ in Fig. 10 corresponds to the situation where two open J' channels are coupled to the reference closed channel $J=2$. A ZWR is still found, but its critical intensity is reduced to about 1.00×10^{13} W/cm^2. As mentioned above, the two coupling strengths of the $J=2\leftrightarrow J'=1$ and $J=2\leftrightarrow J'=3$ transitions are similar; however, their effect is equivalent to the addition of two nearly equal partial widths so that the scaling effect amounts to a reduction of the critical intensity by a factor 2. Finally the four-channel calculation involving also the closed $J=0$ rotational channel produces the curve labeled $J'=0,1,3$. The critical intensity is slightly shifted down to 0.72×10^{13} W/cm^2. A study has also been carried out starting from $J=0$ as the reference closed channel, with extension up to five values of J' and similar conclusions about the survival of ZWRs were obtained.

The concept of control through zero-width resonances thus appears to be robust with respect to variations of the model itself, not just at the level of its parameters, but at the level of its size and complexity, as reflected by the number of channels that are involved in the dynamics. We have explored explicitly the case of the gradual enrichment of the truncated Floquet scheme, as we go from the single-block (two-channel) to a four-block (eight-channel) representation, and the case of an enrichment of the coupled-channel scheme by the inclusion of rotational states. In both cases, there is always one channel that dominates and leads to the ZWR. In this case, it was the ZWR associated with $v=8$ which was preserved, and only its critical intensity was affected by the addition of further coupled channels. In a similar manner, we expect that the inclusion of permanent dipole terms to the time-dependent laser-induced interaction potential matrix in Eq. (2) will merely have the effect of displacing the appearance intensity I_c of this ZWR.

IV. CONCLUSION

In conclusion, we have shown that efficient and selective stabilization can be obtained in strong laser fields through a mechanism which combines the adiabatic transport on a Floquet resonance and the dynamical stabilization of this state in terms of a long-lived ZWR. The *efficiency* of this stabilization scheme rests on a compromise between the adiabatic attainability of the ZWR, and the time that such an adiabatic transport would necessitate. The *selectivity* is related to the fact that different critical intensities characterize different ZWRs which result from the adiabatic transport of corresponding field-free initial vibrational states. In other words, a critical intensity selectively stabilizes a given vibrational state, while the others are dissociating.

The robustness of the overall enhancement of the stabilization through ZWRs, with respect to the dimensionality of the model, has successfully been checked, by partial inclusion of the rotational dynamics. We are now exploring the possibility offered by frequency chirping to modify critical intensities, decreasing their values for a given vibrational state. This would help to improve efficiency by a more favorable compromise between adiabaticity and dissociation during the pulse's rise time. An attractive and promising motivation for such a control scenario remains the production of cold molecules by laser purification of all the rovibrational populations, except the one corresponding to the vibrationally cold ground state.

ACKNOWLEDGMENTS

The authors gratefully acknowledge Professor Arne Keller for fruitful discussions. T.T.N-D. and C.L. acknowledge support by the Natural Sciences and Engineering Research Council of Canada (NSERC).

[1] A. Giusti-Suzor, X. He, O. Atabek, and F. H. Mies, Phys. Rev. Lett. **64**, 515 (1990).
[2] P. H. Bucksbaum, A. Zavriyev, H. G. Muller, and D. W. Schumacher, Phys. Rev. Lett. **64**, 1883 (1990).
[3] A. Zavriyev, P. H. Bucksbaum, H. G. Muller, and D. W. Schumacher, Phys. Rev. A **42**, 5500 (1990).
[4] A. Giusti-Suzor and F. H. Mies, Phys. Rev. Lett. **68**, 3869 (1992).
[5] L. J. Frasinski, J. H. Posthumus, J. Plumridge, K. Codling, P. F. Taday, and A. J. Langley, Phys. Rev. Lett. **83**, 3625 (1999); L. J. Frasinski, J. Plumridge, J. H. Posthumus, K. Codling, P. F. Taday, E. J. Divall, and A. J. Langley, *ibid.* **86**, 2541 (2001).
[6] E. E. Aubanel, J. M. Gauthier, and A. D. Bandrauk, Phys. Rev. A **48**, 2145 (1993); A. D. Bandrauk, E. E. Aubanel, and J. M. Gauthier, in *Molecules in Laser Fields*, edited by A. D. Bandrauk (Dekker, New York, 1994), pp. 109–179.
[7] R. Numico, A. Keller, and O. Atabek, Phys. Rev. A **60**, 406 (1999).
[8] F. Châteauneuf, T. T. Nguyen-Dang, N. Ouellet, and O. Atabek, J. Chem. Phys. **108**, 3974 (1998); T. T. Nguyen-Dang, C. Lefebvre, H. Abou-Rachid, and O. Atabek, Phys. Rev. A **71**, 023403 (2005).
[9] H. Niikura, P. B. Corkum, and D. M. Villeneuve, Phys. Rev. Lett. **90**, 203601 (2003).
[10] C. Lefebvre, T. T. Nguyen-Dang, and O. Atabek, Phys. Rev. A **75**, 023404 (2007).

[11] O. Atabek, M. Chrysos, and R. Lefebvre, Phys. Rev. A **49**, R8 (1994).
[12] O. Atabek, R. Lefebvre, and F. X. Gadea, Phys. Rev. A **74**, 063412 (2006).
[13] A. D. Bandrauk and M. S. Child, Mol. Phys. **19**, 95 (1970).
[14] H. Friedrich and D. Wintgen, Phys. Rev. A **32**, 3231 (1985).
[15] O. Atabek, R. Lefebvre, and T. T. Nguyen-Dang, in *Handbook of Numerical Analysis*, edited by C. Lebris (Elsevier, New York, 2003), Vol. X, p. 745.
[16] M. D. Feit, J. A. Fleck, and A. Steiger, J. Comput. Phys. **47**, 412 (1982).
[17] A. Keller, Phys. Rev. A **52**, 1450 (1995).
[18] R. Heather and H. Metiu, J. Chem. Phys. **86**, 5009 (1987).
[19] A. F. J. Siegert, Phys. Rev. **56**, 750 (1939).
[20] M. Chrysos, O. Atabek, and R. Lefebvre, Phys. Rev. A **48**, 3845 (1993); **48**, 3855 (1993).
[21] N. Moiseyev, Phys. Rep. **302**, 212 (1998).
[22] M. S. Child, *Molecular Collision Theory* (Academic, London, 1974), pp. 53–56.
[23] F. V. Bunkin and I. I. Tugov, Phys. Rev. A **8**, 601 (1973).
[24] M. S. Child, *Semiclassical Mechanics with Molecular Application* (Oxford University Press, New York, 1991), pp. 62–63.
[25] M. S. Child, Mol. Phys. **32**, 1495 (1976).
[26] C. P. Koch, R. Kosloff, and F. Masnou-Seeuws, Phys. Rev. A **73**, 043409 (2006).
[27] J. Weiner, V. S. Bagnato, S. Zilio, and P. S. Julienne, Rev. Mod. Phys. **71**, 1 (1999).
[28] D. A. Varshalovich, A. N. Moskalev, and V. K. Khersonskii, *Quantum Theory of Angular Momentum* (World Scientific, New York, 1998), pp. 130–169.